Numerical simulation on modified chemical vapor deposition (MCVD) thermal flow field

Rubens Cavalcante da Silva
University of São Paulo
São Paulo, Brazil
rubensrcs@usp.br
orcid.org/0000-0002-9794-0992

Paulo Jorge Duda de Morais
University of São Paulo
São Paulo, Brazil
orcid.org/0000-0002-4336-2963

Andre Carvalho
University of São Paulo
São Paulo, Brazil
orcid.org/0000-0001-8569-9532

Wagner de Rossi
Centro de Lasers e Aplicações IPEN-CNEN/SP
São Paulo, Brazil
orcid.org/0000-0003-1371-7521

Claudio Costa Motta
University of São Paulo
São Paulo, Brazil
orcid.org/0000-0002-2508-7320

***Abstract*—This study determines the hydrodynamic and thermal properties of flow field for modified chemical vapor deposition (MCVD) process by means of a computational fluid dynamics (CFD) steady-state simulation. A three dimensional hexahedral mesh and the finite volume method were used to solve the momentum, continuity, energy and chemical species equations on a domain represented by a rotating tube of 24mm diameter, 45 rpm and a flow regime of Re=900. User defined functions were used on STAR-CCM+ code to modeling the $SiCl_4$ oxidation, which occurred in the zones with the highest temperatures (1800K) determined by the torch heating profile. The numerical results were compared with a reference study and a good agreement was obtained.**

***Index Terms*—MCVD, CFD, Finite Volume Method.**

I. Introduction

The modified chemical vapor deposition (MCVD) was developed by [1] and is widely used for the manufacture of high quality optical fiber preforms. This process is based on the high temperature of oxidation of the reagents flowing inside a rotating silica tube and heated by an external heat source as shown in Fig. 1

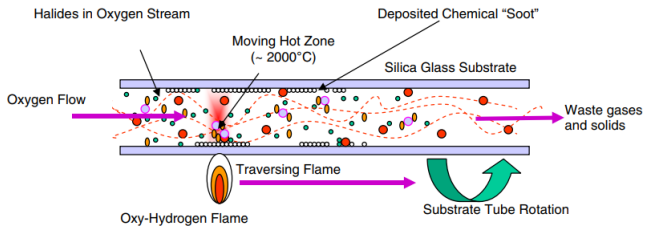

Fig. 1. Schematic representation of the MCVD process [2].

According to [2], in the MCVD process halides (e.g. $SiCl_4$ and $GeCl_4$) within a carrier gas (e.g. O_2 and/or He) are passed into a rotating ultra-pure silica substrate tube. A traversing oxy-hydrogen torch provides the high temperatures needed to oxidize each halide to a corresponding solid – for example, the irreversible reaction between $SiCl_4$ and O_2 described in (1):

$$SiCl_4(g) + O_2(g) \rightarrow SiO_2(s) + 2Cl_2(g) \quad (1)$$

As the heat source moves along the tube, more layers of solid particles are formed and sintered, giving rise to layers of glass with different optical properties. By this process, the resulting optical fiber assumes a variable profile of refractive index along its length, which defines its quality and use as an optical waveguide.

Solid oxide particles move axially with the gases and are deposited on the inner wall of the tube due to thermophoresis; that is, from the net force that a suspended particle experiences in the direction of decreasing temperature in a nonisothermal medium [3]. Nevertheless, an amount of particles formed is not deposited on the wall, and it is lost to the environment. Thus, the correct determination of this deposition efficiency would allow a minimization of production costs, making the industrial process more advantageous.

As the MCVD is a quite complex technological process, the use of numerical tools may present numerous benefits such as provide information that can only be obtained through expensive experiments and increase understanding of the physical phenomena involved. Moreover, the approach used in this work, using a modern CFD code, can be used to simulate a wide range of operational conditions and improve the parameter processes related to MCVD. For instance, for large-mode-area fibers used in high-power laser applications, few parameters of fabrication can be controlled by using numerical tools, such as doping concentration and distribution homogeneity in the fiber core, the solubility of chelates and the designed refractive index profile.

978-1-6654-5273-1/22/$31.00 ©2022 IEEE

This work is organized in 3 sections. The first section presents the mathematical formulation of the problem and the description of the computational procedure. The second section provides the numerical results obtained during the CFD simulation. Finally, the last section presents few considerations on the results and further studies developed to improve the accuracy of the presented model.

II. Theoretical Modeling

The theoretical modeling and boundary conditions of the simulations were based on [4], except by the time regime adopted here (steady-state). The STAR-CCM+ CFD code was used to solve the coupled governing equations. The physical phenomenon considered in this study is the oxidation reaction of $SiCl_4$ carried by a oxygen flow inside a rotating tube, whose wall is heated by an external torch temperature profile.

A. Mathematical Formulation

The three-dimensional steady-state numerical model established to determine the thermal flow field of MCVD process solves the continuity, momentum, energy and species equations, according to Eqs. (2) to (5) respectively, by means of the finite volume method.

$$\nabla . \left(\rho \vec{V}\right) = 0 \tag{2}$$

$$\rho \left(\vec{V} . \nabla\right) \vec{V} = -\nabla p + \mu \nabla^2 \vec{V} \tag{3}$$

$$\rho c_p \nabla T = \nabla . \left(\kappa \nabla T\right) + \Delta H r \tag{4}$$

$$\rho \vec{V} . \nabla Y_i = \nabla . \left(\rho D_i \nabla Y_i\right) - r \tag{5}$$

where $\vec{V}$ is the gas velocity, p is the gas pressure, T is the temperature, ρ is the gas density, κ is the thermal conductivity, Y_i and D_i are the mass fraction and the diffusivity of each chemical specie i (i.e. $SiCl_4$, O_2, SiO_2 and Cl_2), μ is the viscosity, c_p is the heat capacity, H is the enthalpy of the reaction for $SiCl_4$ oxidation and r is an Arrhenius-type reaction rate defined as:

$$r = \left(k_{SiCl_4} \frac{\rho Y_{O_2}}{M_{O_2}}\right) e^{-\frac{E}{RT}} \frac{\rho Y_{SiCl_4}}{M_{SiCl_4}} \tag{6}$$

where k_{SiCl_4} is the pre-exponential Arrhenius rate constant, M is the molecular weight of the chemical species, R is the ideal gas constant and E is the activation energy.

The ideal gas law was incorporated to the model in order to solve the system of equations above [5]:

$$\rho = \frac{pM}{RT} \tag{7}$$

The variables T, $\vec{V}$, p and ρ are solved for the carrier gas and the mass fraction Y_i is solved for each chemical specie i taking into account the oxidation reaction rate r.

B. Computational Domain

The computational domain that represents the rotating quartz tube is a circular cylinder with 24 mm of diameter and 500 mm length. The unstructured hexahedral mesh generated is shown in Fig. 2. The grid spacing varied between 0.5 mm and 1 mm along the whole domain and the total amount of mesh elements was around 350000. Orthogonal prismatic cells layers were generated next to wall surface of the tube to obtain an adequate value of y^+ (Dimensionless wall distance) and accurately predict the boundary layer effects.

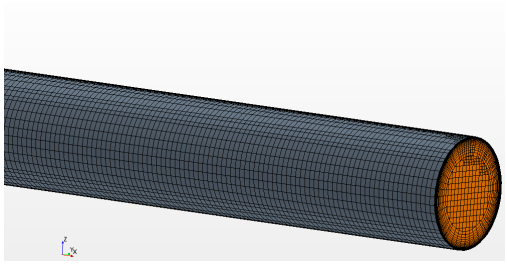

Fig. 2. Unstructured hexahedral mesh of the quartz tube with high density of element near the wall to capture the boundary-layer effects.

C. Boundary Conditions

During the MCVD process, an oxy-hydrogen torch is usually employed to heat the rotation quartz tube, defining the temperature profile of the tube wall. This distribution is important to define the rate and location of the oxidation reaction of halides. The simulations considered as the temperature distribution of the tube wall the profile presented in Fig. 3 whose maximum temperature is 1800 K.

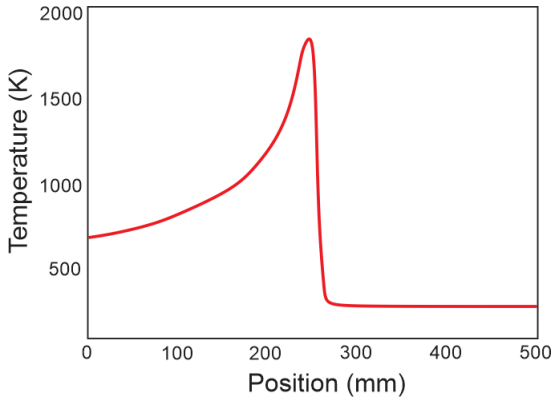

Fig. 3. The axial temperature distribution of quartz tube wall provided by the external torch [4]. The peak of temperature is located at the torch position, i.e., at half tube length.

The study presented here considers only the irreversible oxidation reaction of $SiCl_4$. Moreover, the SiO_2 produced has been treated as a gas due to its the small volume when compared with the total gas inside the domain. The flowrate of carrier gas, O_2, is 2 L/min and the flowrate of $SiCl_4$ is 3 mol/m^3 [4]. During the MCVD process, the initial tempertaure of the gases is 300 K and it is changed as the flow develops

along the tube and heat transfer occurs due to the wall temperature. In addition, the substrate tube rotating at 45 rpm to obtain an homogeneous heating. A schematic representation of the boundary conditions and the domain geometry is depicted in Fig. 4.

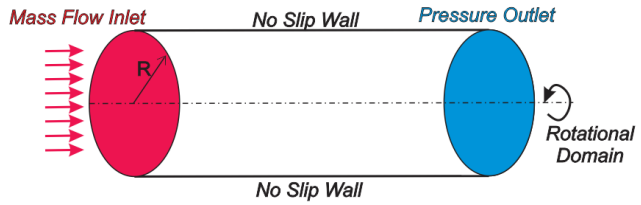

Fig. 4. Boundary conditions and domain geometry of the quartz tube. The mass flow inlet is defined by means of the flow of each chemical specie.

III. Numerical Results

This section presents the results obtained by the CFD simulations. The flow field of the carrier gas was calculated until the convergence criterion was reached, i. e. with the numerical residuals values less than 10^{-4} and negligible variation of the quantities of interest, such as velocity and temperature of the carrier gas, and $SiCl_4$ concentration. To the presented model, the convergence solution was reached after 2100 iterations.

The magnitude of the velocity field of the carrier gas is shown in Fig. 5. One can observe that the region of highest velocities is located at the torch position (dashed line), where the radial profile of the temperature is depicted. After the torch position, is possible to observe the change in the velocity magnitude due to the sharp decrease in the torch temperature profile. In addition, the velocity profile along the tube length, represented by the red lines on the top of Fig. 5, varies according to a Poiseuille-type flow deformed by the effect of the carrier gas temperature variation.

The calculation of the velocity field is important to correctly modeling the MCVD process. During the deposition process of the oxidation, the axial velocity of the resulting particles is identical to that of the carrier gas. On the other hand, its radial velocity always depends on the thermophoresis caused by temperature gradient.

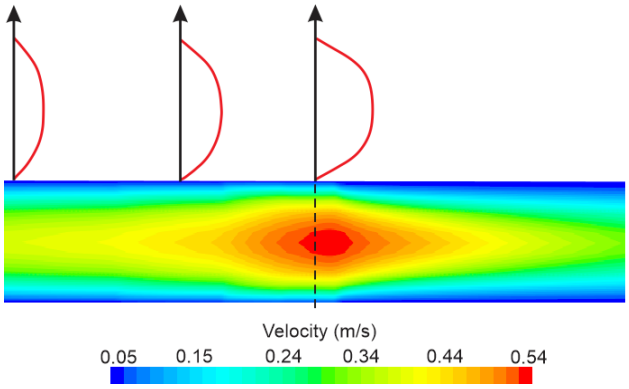

Fig. 5. Velocity field and velocity profiles (top) of the carrier gas along the tube length. At the center of the tube, the velocity profile is well developed and assumes a parabolic shape as a typical Poiseuille flow pattern.

In addition, the longitudinal and radial temperature field of the carrier gas heated by the external torch temperature profile are presented in Fig. 6. The maximum temperature is restricted in the small region near the wall and it is convected through the gas. The center of the tube is where there are the lowest temperatures and the oxide particles suffer small effect of thermophoresis forces (due to negligible temperature gradients), and therefore occurs less deposition of particles. In this sense, the correct modeling of this region is mandatory to improve the calculation of the overall efficiency of the MCVD process .

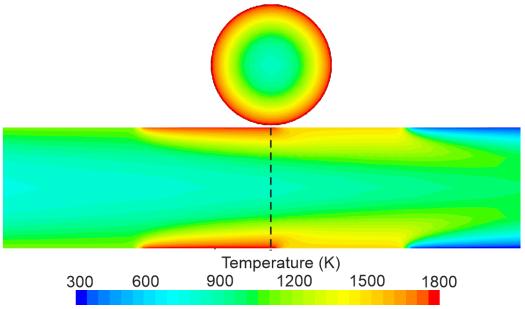

Fig. 6. Longitudinal and radial (top) temperature field of the carrier gas due to the torch temperature profile. The Highest temperature values is presented at the torch position, and the lowest values at the longitudinal center of the tube.

The analysis of the heat transfer results was developed by comparison with the data provided by [4], where the authors calculated the temperature field of the flow, as well as the concentration of $SiCl_4$ and its conversion rate in Fig. 7. It can be seen that the heated zone corresponds to the chemical reaction zone, and the low temperature at the front of the torch is the solute diffusion zone. Meanwhile, the highest temperature corresponds to the highest conversion rate of $SiCl_4$, and the conversion rate of $SiCl_4$ is as high as 96% when the inner wall temperature is around 1800 K. As the temperature decreases from the wall to the fluid center, the $SiCl_4$ conversion rate decreases, and the total conversion rate is 39% [4].

On the other hand, the numerical results for the gas temperature, $SiCl_4$ concentration and $SiCl_4$ conversion rate obtained in this study, hilighting the region near the torch position, are shown in Fig. 8, where one can see some similarities with the data depicted in Fig. 7. The reaction zone, represented by the highest conversion rate in Fig. 7 (c), is located near the torch position, where it also presents the highest temperatures. The evolution of the concentration of $SiCl_4$ concentration is consistent with the expected dynamics of the chemical phenomenon: it decreases as the convertion rate of $SiCl_4$ rises (whose highest values are in the region right before the torch position, i. e., the reaction zone).

In order to provide a comprehensive observation, the evolution of dimensionless concentration of chemical species along the vertical diameter at the half section of the tube is presented in Fig. 9. The reference value for the dimensionalization is the concentration of $SiCl_4$ at inlet. As the temperature increases

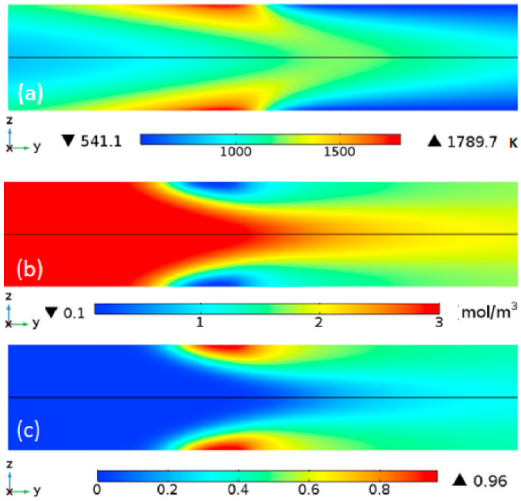

Fig. 7. The distribution of internal fluid temperature (a), $SiCl_4$ concentration (b) and $SiCl_4$ conversion rate (c) [4].

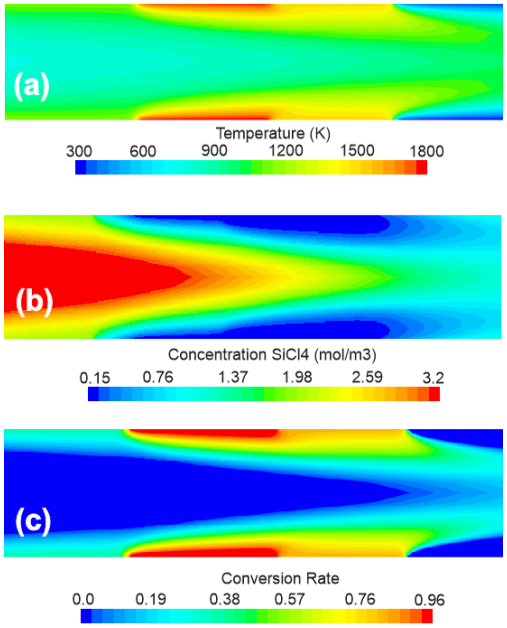

Fig. 8. Simulation results for the distribution of internal fluid temperature (a), $SiCl_4$ concentration (b) and $SiCl_4$ conversion rate (c). Note that the highest conversion rate is located in the region around the torch position

downstream, the $SiCl_4$ oxidation reaction is initiated (near the wall) and the SiO_2 concentration increases. In this sense, the higher concentration of the resulting oxide is found near the tube wall and decreases radially, presenting a minimum value at the center of the tube.

Nevertheless, it is important to consider few points of attention, specially regarding to the calculation of concentration of $SiCl_4$ and the reaction rate definition. The region of lower concentration of halide (near the tube wall) is wider than that presented in Fig. 7 (b), as well as the corresponding region of reaction rate. Those observations suggest that some improvements should be made in the model, specially regarding to

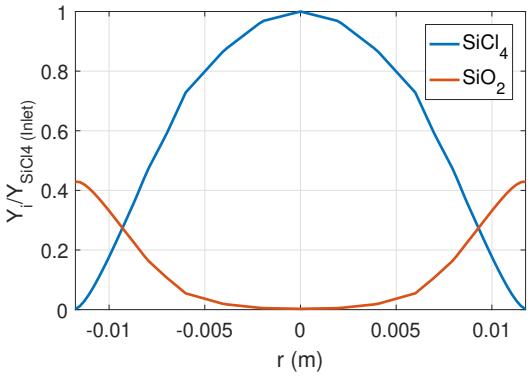

Fig. 9. Distribution of dimensionless concentrations of $SiCl_4$ and SiO_2 along the central vertical diameter at half length tube section. The curves indicate that the highest production of oxide occurs near the wall, where the temperature is maximum, as well as the chloride concentration is minimum, which demonstrates that this specie is being consumed during the formation of the oxide particles.

reaction coefficients in the Arrhenius rate.

IV. Concluding Remarks and Ongoing Work

A steady-state numerical analysis of heat transfer and fluid flow has been carried out for modified chemical vapor deposition (MCVD) process. The results presented good agreement with the reference data. The velocity and temperature fields of the carrier gas were adequately solved and the region where the oxidation of $SiCl_4$ occurred (right before the torch position) presented the righest reaction rates.

Some modification in the model is being implemented in order to improve the ranging of the chemical results, such as to include other species in the process (e.g. $GeCl_4$) and analyze the influence of different external torch temperature profile on the rate of chemical reactions. The correct definition of the reaction zone and the temperature and velocity fields is important to adequately modeling the MCVD process and evaluate the efficiency of deposition of the resulting particles oxide.

Further studies on the modeling of oxidation reaction of $SiCl_4$ and $GeCl_4$ are being developed in order to make the model more complete and realistic. The dynamics of oxide particles are being evaluated in a lagrangean multiphase interaction model to predict their behavior and the deposition pattern along the substrate tube, which will make the model more capable to calculate the refractive index profile of the resulting optical fiber.

References

[1] J. B. Macchesney, P. B. O'Connor and H. M. Presby "A new technique for the preparation of low-loss and graded-index optical fibers,"Proceedings of the IEE, 1974.

[2] C. K. W. Cheung, D. Haley, D. F. Fletcher, G. W. Barton and P. McNamara "Simulation of particle–vortex interactions in the modified chemical vapor deposition process,"Journal of Non-Crystalline Solids, 353, pp. 4066—4075, 2007.

[3] K.S. Park, M. Choi and J.D. Chung "Unsteady heat and mass transfer on the codeposition of SiO_2/GeO_2 during the modifed chemical vapor deposition process,"International Journal of Heat and Mass Transfer, vol. 43, pp. 3209—3217, 2000.

[4] Y. Zhang, N. Liu, X. Li, F. Chen, B. Yang, C. Gao, D. Pan and B. Li "Simulation of unsteady thermal-flow field for modified chemical vapor deposition (MCVD) process,"International Journal of Thermal Sciences, 172, pp. 1—8, 2022.

[5] S. Joh, and R. Greif "The effects of $SiCl_4$ and $GeCl_4$ oxidation, variable properties, buoyancy and tube rotation on the modified chemical vapor deposition process,"International Journal of Heat and Mass Transfer, vol. 34, 10, pp. 1911—1921, 1995.